

# Making Every Frame Matter: Continuous Activity Recognition in Streaming Video via Adaptive Video Context Modeling

Hao Wu  
Nanjing University

Donglin Bai  
Microsoft Research

Shiqi Jiang  
Microsoft Research

Qianxi Zhang  
Microsoft Research

Yifan Yang  
Microsoft Research

Xin Ding  
Microsoft Research

Ting Cao\*  
Microsoft Research

Yunxin Liu  
AIR, Tsinghua University

Fengyuan Xu  
Nanjing University

## Abstract

Video activity recognition has become increasingly important in robots and embodied AI. Recognizing continuous video activities poses considerable challenges due to the fast expansion of streaming video, which contains multi-scale and untrimmed activities. We introduce a novel system, CARS, to overcome these issues through adaptive video context modeling. Adaptive video context modeling refers to selectively maintaining activity-related features in temporal and spatial dimensions. CARS has two key designs. The first is an activity spatial feature extraction by eliminating irrelevant visual features while maintaining recognition accuracy. The second is an activity-aware state update introducing dynamic adaptability to better preserve the video context for multi-scale activity recognition. Our CARS runs at speeds  $>30$  FPS on typical edge devices and outperforms all baselines by 1.2% to 79.7% in accuracy. Moreover, we explore applying CARS to a large video model as a video encoder. Experimental results show that our CARS can result in a 0.46-point enhancement (on a 5-point scale) on the in-distribution video activity dataset, and an improvement ranging from 1.19% to 4% on zero-shot video activity datasets.

## 1. Introduction

Video activity recognition [7, 16, 26, 37, 42, 48] is an important and long-standing application. These tasks are widely used in advanced human-computer interactions (HCI), including robotics and augmented reality [9, 11, 35]. To enable advanced HCI, real-time recognition of streaming video on resource-constrained mobile or edge devices is



Figure 1. An example of continuous video activity recognition in streaming video. CARS takes every frame as input and continuously recognizes human activities.

crucial. Activity recognition relies heavily on video context, making it difficult to determine actions from a single frame. Therefore, a continuous video activity recognition system must maintain video context, allowing it to infer activities in new frames based on the accumulated context. However, achieving efficient continuous recognition in streaming video is challenging for the following reasons.

**(i) Diverse Temporal Scales of Activities.** Continuous video activity recognition needs to capture the spatio-temporal features of activity on multiple temporal scales [30, 46]. As shown in Figure 1, activities at different scales may have dependencies or causal relationships, such as taking bread from a bag as part of making a sandwich. The system must continuously recognize activities of varying lengths based on newly received video frames.

**(ii) Accumulating Redundancy in Streaming Video.** Continuous video activity recognition normally needs to capture meaningful features from the raw streaming videos, which are dominated by noise and redundancy. As illustrated in Figure 5, activity-related pixels are sparsely distributed in the video. Without effective online reduction, the accumulation of redundant features can quickly overwhelm the activity-related features as the video progresses.

**(iii) Computational Efficiency Under Resource Con-**

\*corresponding author

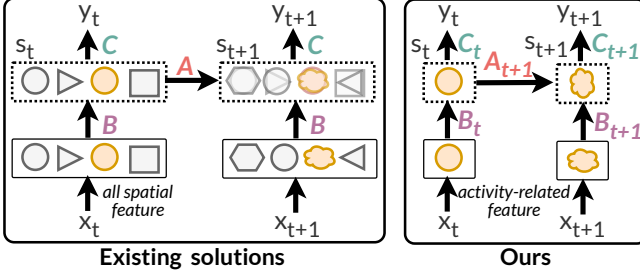


Figure 2. Difference between our idea and existing solutions on maintaining the hidden state.

**straints.** Continuous video activity recognition must guarantee a timely recognition of the scene while managing the resource constraints of typical edge devices. For instance, robots or embodied AI [9] systems must continuously perceive dynamic scenarios through streaming video input to carry out reasoning [35] and task planning [11].

Existing video recognition efforts have explored numerous strategies for maintaining video context, yet none have been able to address all the challenges simultaneously. Works, using “all frames at once” strategy (Figure 3(a)), perform activity recognition on every frame of the video, which theoretically yields the highest accuracy [10, 19]. However, its efficiency is the biggest concern. Other works use “sliding window” strategy (Figure 3(b)) to reduce computational cost [17, 21–23]. However, these methods struggle to accurately recognize activities at different scales. Some approaches use a “hidden state assistance” design (Figure 3(c)), where a hidden state compresses video context to enable more efficient activity recognition. However, existing state-assisted methods do not effectively eliminate spatiotemporal redundancy in the streaming video, resulting in inefficient utilization of the hidden state and low accuracy.

The all-frame-at-once approach suffers from efficiency degradation over time as data volume grows, while the sliding window method often faces challenges in selecting optimal window sizes or sampling strategies, compromising accuracy. Therefore, our design builds on the existing state-assistant framework, which is efficient—processing one frame at a time—and accurate—adaptively maintaining video context through carefully designed hidden states. As illustrated in Figure 2, we argue that existing state-assistant works lack activity-aware design in both temporal and spatial dimensions. They tend to compress all video features, including the redundant background features, into the hidden state, resulting in inefficient use of hidden states, poor preservation of video context, and low recognition accuracy. Our core idea is to *selectively compress only activity-related features in temporal and spatial dimensions, which we name adaptive video context modeling*.

In this paper, we propose CARS for continuous video

activity recognition in the streaming video, utilizing the adaptive video context modeling, with two key designs. **First, activity spatial feature extraction** (Section 3.1). To reduce redundant visual information, we employ a *data reduction strategy that operates without requiring supervision from masks or bounding boxes of activity-related features*. During training, we maximize feature elimination from the video input while preserving recognition accuracy. This adversarial learning process allows our CARS to discard spatial features irrelevant to the activity. **Second, activity-aware state update** (Section 3.2). Existing methods struggle to effectively maintain video context for multi-scale activities. Our design integrates a *dynamic adaptability, akin to the attention mechanism in transformers*. We dynamically recalculate the weight parameters based on the current input frame during the input processing, hidden state update, and output generation.

We evaluate CARS across various activity recognition tasks, comparing it with widely-used models for video recognition. Results show that with significantly fewer trainable parameters (ranging from 8.5k to 34.1M less than the baselines), CARS achieves accuracy improvements of 1.2% to 79.7% over baseline methods. Regarding latency, we evaluate CARS on typical edge devices (NVIDIA Jetson Orin, Apple MacBook, and an Intel PC with NVIDIA 4090 GPU). It achieves >30FPS on all these devices, up to 20× faster than the available inference systems.

To further explore the capability of our design, we apply CARS as a video encoder to a large video model to improve its activity recognition capability (Section 5). Specifically, we replace the visual encoder of the SOTA large video model VideoLlama2 [8] by CARS. The results demonstrate a 0.46-point improvement (on a 5-point scale) on the in-distribution dataset, and an improvement ranging from 1.19% to 4% on zero-shot datasets.

**Contribution.** We summarize our contribution as follows:

- We propose a continuous video activity recognition system, CARS, based on adaptive video context modeling. It promptly recognizes the activities in incoming video frames by efficiently maintaining video context for multi-scale activities.
- Our CARS incorporates two key techniques to enhance the utilization efficiency of hidden states, i.e., minimizing redundancy from activity-irrelevant spatial information, and improving adaptability to streaming input while maintaining state.
- Experiments show that CARS surpasses all baselines in streaming video activity recognition, using fewer parameters and achieving over 30 FPS on typical edge devices, which can enable on-device video recognition for embodied AI. We also showcase that CARS can enhance the large video models by serving as the video encoder.

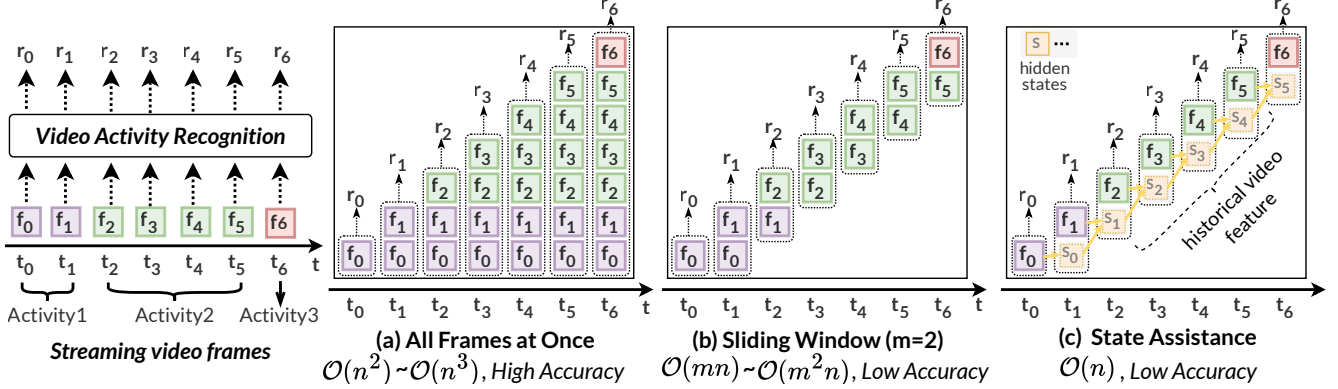


Figure 3. Typical designs for streaming video activity recognition. The “All Frames at Once” design processes all video frames at every moment. The “Sliding Window” design incorporates only the latest (or sampled)  $m$  frames. The “State Assistance” relies on a single frame at a time and maintains video context through a hidden state.

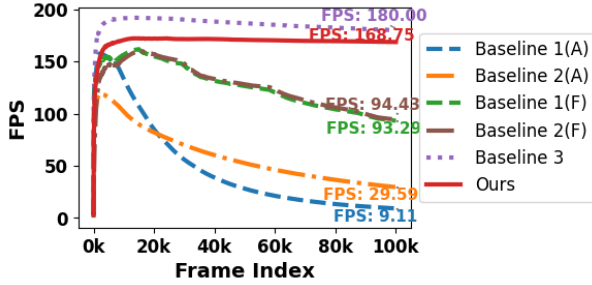


Figure 4. Processing speed of video activity recognition on RTX4090 (a 100k-frame video). Baselines 1(A) and 2(A) represent Transformer and Convpooling-based solutions using the “All Frames at Once” design. Baselines 1(F) and 2(F) employ the “Fixed window size” design (the window size is 100). Baseline 3 denotes an LSTM-based “State Assistance” design.

## 2. Background & Related Works

Various approaches strive to achieve continuous activity recognition, but none have solved this challenging task.

**All Frames at Once.** A straightforward method is to input all the past frames into the model at each time step, as illustrated in Figure 3(a). However, it is certainly too costly for model inference and training. Take a Transformer model as an example, with the number of streaming frames  $n$  grow, the computation cost of video activity recognition is  $\mathcal{O}(n^3)$ . Even with the many linear alternatives of Transformers, such as Linformer [41], RetNet [36], Mamba [13], and RWKV [28], the cost is still  $\mathcal{O}(n^2)$ . Our experiment (Figure 4) shows that as frames increase, FPS drops to 0.05 times, a 95% decrease.

**Fixed Window Size.** The most commonly used technique to control the cost is to fix the input size of the model even with the growing number of frames, such as sliding window or sampling [17, 21–23], shown in Figure 3(b). For example, TSN [40] first divides the past video into seg-

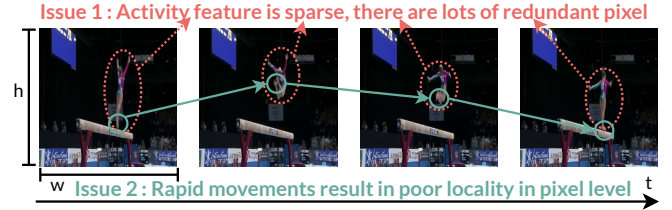


Figure 5. Video frames of the balance beam sports, selected from the FineGym99 dataset [30]. The entire gymnastic movement was captured in only 17 frames, lasting less than 700 milliseconds.

ments and selects a random snippet from each segment for activity recognition. VideoLlama2 [8] only samples 8 or 16 frames as input for any video length. This method has to ignore many detailed features. VideoMamba [20] adopt the Mamba [13] as the architecture to perform the efficient video understanding, however, it still adheres to the batch-based processing strategy. *The main challenge is selecting an optimal window size to balance the detection of both short and long activities.*

**State Assistance.** There are also works [15, 32, 47], shown in Figure 3(c), that only input one current frame into a model (e.g., CNN) first to extract spatial features, and then conduct feature aggregation (e.g., through pooling [18] or LSTM [14]) among frames over time to capture temporal dependencies by hidden states. By maintaining a group of hidden states, this method significantly enhances efficiency by reducing complexity to approximately  $\mathcal{O}(n)$  [15, 32]. However, *as the input size grows, the fixed-size state struggles to remember the increasing history of inputs* [30, 40].

## 3. CARS Design

**A motivating video sample.** Video streams contain both spatial (within-frame) and temporal (between-frame) information, both critical for accurate recognition. Fig-

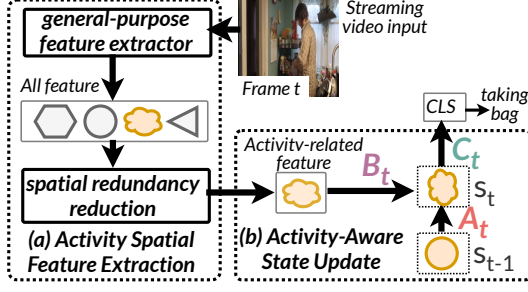


Figure 6. CARS’s workflow for continuous activity recognition via adaptive video context modeling by selectively compressing only activity-related features into the hidden state.

Figure 5 presents a video sample from a real-world gymnastics match to motivate our design and explain the challenges we faced. There are two issues we can observe from the video sample. **Issue 1:** the activity-related spatial feature is sparse. The activity feature in a video sample may be captured by only a small portion of the pixel content. **Issue 2:** object movement causes poor locality at the pixel level. It is hard to accurately recognize activities merely by analyzing two adjacent regions (by setting thresholds).

We have observed the efficiency advantages of state-assistant methods in handling streaming video. Therefore, we utilize a state-assistant design, which involves recurrent updates over a sequence through hidden states [33]. Our CARS has two key designs, i.e., activity spatial feature extraction and activity-aware state update, to solve these two issues. Figure 6 illustrates the system workflow.

During the usage, streaming video is continuously input into the system frame by frame (without sampling). Our CARS extracts activity-related features and sends them to the activity-aware state update module. During the state update, the system attempts to identify possible activities and uses the activity features to update the corresponding part of the hidden state. If no further activity features related to those features maintained in the hidden state arrive, the corresponding video context is cleared from the hidden state. The updated state is stored in the system, waiting for the next frame to update it. Simultaneously, the updated hidden state can be sent to a classifier for timely activity recognition. With our optimization, the entire system can perform real-time video activity recognition on typical edge devices.

### 3.1. Activity Spatial Feature Extraction

The **challenge** of addressing issue 1 is that we *lack supervised data to differentiate between redundant spatial features and those relevant to activities*. Because the types of activities in the real world are diverse. We cannot merely retain an object’s pose and position. For instance, in Figure 5, it is crucial to also keep the feature of the balance beam present in the environment. In this way, we can accu-

rately comprehend that this is a gymnastics activity, rather than a simple jump.

The *core idea* of our feature extraction is to utilize the information bottleneck [38] as an *unsupervised method* to extract task-specific features. Specifically, we employ an information reduction module aimed at minimizing input features while maximizing task accuracy during training. Through this adversarial constraint, it can reduce redundancy and effectively achieve activity-related feature extraction.

Formally speaking, let  $X$ ,  $X'$ , and  $Z$  denote the random variables that represent all spatial features, extracted activity-related features, and redundant features, respectively. In our scenario, the activity spatial feature extraction determines how the feature  $X'$  is extracted from  $X$  for the recognition task  $f_\theta$ . The goal of the activity-related feature extraction is to minimize the inclusion of redundancy information  $Z$  in extracted feature  $X'$  while ensuring maximum data utility, i.e.,

$$\min_{\mathcal{I}(X'; Z) < \epsilon} \|f_\theta(X'), f_\theta(X)\|, \quad (1)$$

where  $\mathcal{I}$  is the mutual information to quantify the amount of information obtained about one random variable by observing the other random variable.  $\|\cdot, \cdot\|$  is used to measure the distance between two variables.

However, given the lack of supervised data regarding redundant information  $Z$ , it is hard to minimize the  $\mathcal{I}(X'; Z)$ . Note that,  $\mathcal{I}(X'; Z) \leq \mathcal{H}(X')$ , where  $\mathcal{H}$  is the entropy of a random variable. So, we have the relaxation of Equation 2, i.e.,

$$\min_{\mathcal{H}(X') < \epsilon} \|f_\theta(X'), f_\theta(X)\|. \quad (2)$$

That is, by minimizing the information of extracted features  $X'$  and preserving the accuracy of activity recognition, we can remove the redundant features as much as possible. Please note that the data utility objective,  $\min \|f_\theta(X'), f_\theta(X)\|$ , is optimized by the accuracy of the activity recognition task (Equation 5).

To reduce the information entropy of extracted features  $X'$ , we propose two steps, i.e., the pooling layer and an information funnel. Specifically, in our activity spatial feature extraction module, we first a pre-trained powerful feature extractor, i.e., CLIP [29], to extract general-purpose spatial features from an input frame. The CLIP model divides the input frame into multiple patches and computes an embedding for each patch. We utilize the average pooling to aggregate these embeddings by computing their mean, generating a single embedding. This constitutes the *first* stage of information reduction for  $X'$ . After the first stage, each frame is reduced to a single embedding. Subsequently, this embedding is passed through our information funnel, which consists of a linear layer followed by an activation function, where the output size of the linear layer is smaller than its



input size. This completes the *second* stage of information reduction for  $X'$ .

### 3.2. Activity-Aware State Update

The **challenge** of addressing issue 2 lies in *online associating the features of each incoming frame with those in the video context, i.e., hidden state*, thereby enhancing recognition accuracy. This state update serves as the association process since the recognition results are based on the updated state.

We take the RNN as an example to introduce the traditional state update. It computes  $y$  through a dynamic recurrence of input signals  $x$  at each time step  $t$  through hidden states  $s$ . Formally,

$$\begin{aligned} s_t &= \phi_h(\mathbf{A}s_{t-1} + \mathbf{B}x_t + \mathbf{b}_h), \\ y_t &= \phi_o(\mathbf{C}s_t + \mathbf{b}_o). \end{aligned} \quad (3)$$

where  $\mathbf{A}$ ,  $\mathbf{B}$ , and  $\mathbf{C}$  denote the state matrix, input matrix, and output matrix, respectively. The  $\mathbf{b}$  denotes the bias parameters, and the functions  $\phi$  denotes activation functions.

However, the RNN and its gating-based variants, e.g., LSTM [31], are widely considered challenging to maintain input context by many research works [12, 27, 45]. Our experimental results indicate that the LSTM-based baseline performs poorly on streaming video inputs (Table 2). We argue that the underperformance of such methods is due to their inefficient utilization of the hidden state. Specifically, standard RNN processes input at different moments identically, i.e., fixed  $A$ ,  $B$ , and  $C$  in Equations 3, leading to irrational use of the hidden state (Figure 2).

We argue that this deficiency stems from the state update method’s inability to adapt effectively to incoming video frames, as it applies one update strategy to all frames, irrespective of their distinct features. We enhance the state update method by enabling activity-aware hidden state updates based on activity spatial features. The *core idea* is to introduce *dynamic adaptability, akin to the attention mechanism in transformers*, which adjusts its focus across input sequences to accommodate varying inputs.

Specifically, we replace the fixed matrix used for state updates with an input-dependent update manner. Our input-dependent update takes the current activity spatial features as input and determines how the current input should be incorporated into the hidden state. Formally,

$$A \rightarrow A_t = f_A(x_t); B \rightarrow B_t = f_B(x_t); C \rightarrow C_t = f_C(x_t). \quad (4)$$

That is, during training, *we no longer learn the  $A$ ,  $B$ , and  $C$  matrices directly but instead learn how to dynamically generate these matrices based on the input.*

Here, we employ Mamba [13] as the implementation of our activity-aware state update module, as it aligns with our design philosophy: it dynamically computes these matrices

---

**Algorithm 1:** The parallel training structure of CARS.  $\theta_{\text{spatio-encoding}}^*$  is frozen during the training.

---

**Data:** Video frames and corresponding labels:  $X_{1:n}$  and  $Y_{1:n}$

**Result:** Trained parameters:  $\theta$

```

1 begin
2   while not convergent do
3      $\text{Emb}_{1:n} \leftarrow \theta_{\text{CLIP}}^*(X_{1:n})$ 
4      $\text{Tok}_{1:n} \leftarrow \theta_{\text{extractor}}(\text{Emb}_{1:n})$ 
5      $\text{Ir}_{1:n} \leftarrow \theta_{\text{state.maintenance}}(\text{Tok}_{1:n})$ 
6      $\hat{Y}_{1:n} \leftarrow \theta_{\text{cls}}(\text{Ir}_{1:n})$ 
7      $L \leftarrow \mathcal{L}(Y_{1:n}, \hat{Y}_{1:n})$ 
8      $\theta \leftarrow \theta - \nabla_{\theta} L$ 
9   return  $\theta$ 
```

---

based on each input. Additionally, Mamba’s implementation accelerates the training process for such recursive formulations. Note that while Mamba has been explored for video processing [7, 8, 20], these works adopt strategies such as processing “all frames at once” or using a “fixed window size”, treating Mamba primarily as a lightweight alternative to Transformers. In contrast, our “state-assistant” design fundamentally differs in both approach and purpose.

### 3.3. Training Structure

The training structure is detailed in Algorithm 1. The CARS’s architecture consists of a pre-trained vision encoder ( $\theta_{\text{CLIP}}$ ), a feature extractor ( $\theta_{\text{extractor}}$ ), an activity-aware state update module ( $\theta_{\text{state.maintenance}}$ ), and a classifier ( $\theta_{\text{cls}}$ ). The vision encoder extracts the general-purpose spatial feature and is frozen during training. The feature extractor is a linear layer with ReLU activation. The activity-aware state update module is a single Mamba layer. The classifier is a ReLU activation.

The loss function  $\mathcal{L}$  is a frame-weighted loss. The core intuition is that activity recognition can be categorized into two types: *motion-focused* (requiring temporal information, e.g., performing a triple somersault) or *scene-focused* (relying solely on static information, e.g., drinking water). Formally, it can be expressed as:

$$\mathcal{L}_v = W^T \times [\mathcal{L}_f^1, \mathcal{L}_f^2, \dots, \mathcal{L}_f^N], \quad (5)$$

where  $W$  is the weight vector of the loss from Frame 1 to Frame  $N$ . For motion-focused tasks, we recommend a linear growth strategy, where the weight of the loss for the initial frame is relatively low and gradually increases over time within the video frames. Specifically,  $W = [\frac{i}{N^2}]_{i=1}^N$ . Conversely, for scene-focused datasets, a uniformly weighted approach is recommended. That is,  $W = [\frac{1}{N}]_{i=1}^N$ .

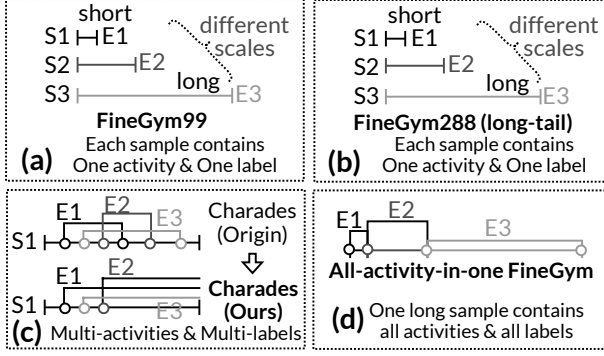


Figure 7. Datasets used in experiments. S represents a sample; a line segment represents the duration of an activity; E represents a label. In Charades, a frame may have multiple labels.

## 4. Evaluation

**Hyperparameter Setting.** The AdamW [24] is adopted as the optimizer. The learning rate changes dynamically, using Cosine annealing with warm restarts. This method adjusts the learning rate between  $1e-3$  and  $1e-6$  every 10 epochs. Aside from these adjustments, the other hyperparameters are kept at their default settings as provided in PyTorch v2.2.0. Regarding the training process of the network, it requires approximately 100 to 200 epochs to converge in different datasets. We train these models on a server with 8 RTX4090 GPU cards, and it takes about 3 to 6 hours to train a model on different datasets.

**Optimization Deployment.** We implemented the CLIP vision encoder using the llama.cpp framework [2], performing INT8 quantization for improved efficiency. While the CLIP.cpp framework [1], based on llama.cpp, only supports CPU backends, limiting GPU use on mobile devices, other frameworks like OpenClip [5] and ONNXRuntime-GPU [4] also lack support for Jetson GPUs. We extended support for ggml format, enabling GPU-based inference across all platforms, which resulted in a significant performance boost (see Figure 9). Furthermore, we compiled the Mamba implementation [3], which originally supported only PyTorch with CUDA, into ggml format for cross-platform deployment. Through these optimizations, we successfully deployed our CARS on a MacBook Air (M3, 2024), Jetson AGX Orin 64GB, and a PC with an RTX 4090 GPU.

### 4.1. Experiment Setups

**Evaluation Goals.** We aim to evaluate **four capabilities**:

- Capability 1:* Recognition of activities across timescales.
- Capability 2:* Activity Recognition in streaming input.
- Capability 3:* Prompt response as more frames are received.
- Capability 4:* Generality for long-tail activities.

**Datasets.** We utilize five datasets to evaluate different capabilities. *FineGym99* [30] (For capabilities 1 & 3). It is a gymnasium video dataset. Each video clip is labeled with

a gymnastics movement. The duration of activities varies from 2 to 50 seconds. *FineGym288* [30] (For capabilities 1, 3, & 4). It is an extended version of FineGym99, which enhances its by adding categories. FineGym288 has a natural long-tail distribution.

*Charades* [34] (For capabilities 1 & 3). It is a multi-label dataset, composed of daily indoor activities with an average length of 30 seconds. Each video clip consists of about 800 frames on average, varying from 32 to 3,944 frames. We re-annotated Charades, as Figure 7(b), to evaluate the method’s effectiveness in maintaining video context when multiple activities occur simultaneously.

*All-activity-in-one FineGym* (For capabilities 1, 2, & 3). It is constructed based on the FineGym99 as shown in Figure 7(c). We concatenated all the video clips from FineGym99’s testing dataset, forming a single long video lasting 3.5 hours and consisting of over 440k frames. The concatenated video is employed to simulate streaming video containing continuous activities.

**Baseline Methods.** We utilize five baselines to execute continuous perception, whereby the method predicts an outcome at each timestep. Baselines 1, 2, and 3 are constructed following different video processing paradigms (as shown in Figure 8). Their overall architecture *mirrors ours*, except that we replace the mamba layer with other networks. *Baseline 1* utilizes a Transformer [39]. *Baseline 2* utilizes a convPooling [18], which consists of a 1D convolution and a 1D adaptive max pooling. *Baseline 3* utilizes an LSTM [14].

Baselines 4 and 5 are state-of-the-art (SOTA) methods for balancing accuracy and efficiency for video classification for on-device computing scenarios. *Baseline 4:* MoviNetA0 [19]. This is a Mobile Video Network specifically designed for efficient video recognition. This method applies down-sampling when processing videos. Drawing from the experience of using this model on the Charades dataset, we similarly down-sample the video to 6 fps for video preprocessing. *Baseline 5:* Mvitv2[22] This is an improved multiscale vision transformer for both classification and detection tasks. This method necessitates the sampling of any given video to a fixed number of frames for video classification tasks. We trained the baseline that takes as input 16 frames at a time, which is one of the default settings.

**Input Strategy.** We utilize three typical input strategies to perform the evaluation.

- S1: All frames feeding.* All frames from frame 1 up to frame  $N$  are fed into the baseline method to provide the necessary context for achieving continuous perception at timestep  $N$ .
- S2: Sliding windowed feeding.* All frames between the  $(N - m)$ -th frame to the  $N$ -th frame are fed into the baseline at timestep  $N$ , where  $m$  denotes the sliding window size.
- S3: Single frame feeding.* Only frame  $N$  is supplied to the baseline method.

**Metrics.** In this work, we utilize various metrics, namely

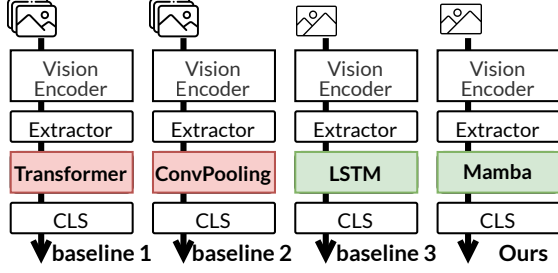


Figure 8. The constructed baselines 1, 2, and 3.

Accuracy, Mean Average Precision (mAP), and the Jaccard Index for single-label and multi-label video classification tasks. Furthermore, we introduce a novel metric referred to as the *Early Detection Rate (EDR)*, designed to evaluate the model’s ability to detect activities promptly within videos. The definition is  $EDR = (E_{pred} - E_{gt}) / E_N$ , where  $E_{pred}$  refers to the frame index at which the label is detected.  $E_{gt}$  represents the ground truth frame index, that is, the index of the frame where the activity begins.  $E_N$  signifies the total number of frames in the activity.

## 4.2. Evaluation of All Capabilities

In Table 1, we present the outcomes from several baseline models across different datasets. We first introduce each column’s meaning and statistical methods, followed by an evaluation of our methodology and findings.

The #Param column signifies the size of a model’s parameters. Owing to the varying category numbers in the three datasets, there is a marginal difference in the parameter count in the final layer for different tasks, approximately a 10k difference in parameters. Here, we reference the parameter count when classifying the FineGym99 dataset. Baselines 1, 2, and 3, as well as our model, all utilize the same CLIP model with a parameter size of 149M. When excluding the CLIP, our design exhibits the smallest parameter count.

We chose the most natural input strategy for each baseline to assess the accuracy. For batch-based methods, i.e., Baselines 1, 2, 4, and 5, we adopted the all-frame feeding strategy. Although this significantly increases computational overhead, it enables these methods to have sufficient context to recognize the video activities. Both Baseline 3 and our method utilize a streaming processing paradigm, for which we selected the single-frame feeding strategy.

In evaluating single-label classification datasets, we utilize Accuracy (Acc) as the primary measure of correctness. This accuracy is ascertained by verifying whether the correct action is detected within a given video. The EDR is calculated as introduced in Section 4.1 (Metrics). When dealing with multi-label classification datasets, two variants of mean Average Precision (mAP) are employed to gauge correctness. The  $mAP_{all}$  metric is determined by considering

predictions of all frames in the video. The  $mAP_{last}$  entails calculations based solely on the prediction results of the final frame in the video. It’s important to note that the label of the last frame includes labels for all actions present within the current video. Each label’s EDR is computed separately and then averaged. If a method fails to detect a particular label, this failure is taken into account during computation by adding a 100% increase to the result for that category. This signifies that the correct label was undetected even after the video’s conclusion. Below we present our experimental analyses and the subsequent conclusions:

**Superior Accuracy:** Our method consistently outperforms all baseline methods in terms of accuracy across all tasks, improving metrics by ranges of 2 to 79.7, 2.9 to 78.2, 1.2 to 14.5, and 0.7 to 16.3. The leading accuracy demonstrates that our CARS can effectively recognize activities of different scales (*Capability 1*). The superior accuracy on the FineGym288 dataset underscores our method’s generalization ability for long-tailed data (*Capability 4*).

**Prompt Recognition :** Our approach exhibits an outstanding ability to promptly detect activities (*Capability 3*) and continuously process (*Capability 2*) by EDR. For single-label tasks, activities are detected within the first quarter of their occurrence. For complex multi-label tasks, all activities are identified halfway through the video.

**Optimal Use of Trainable Parameters:** Notably, our method retains superior performance while utilizing a minimal number of training parameters, amounting to only 202K. This represents a drastic reduction when compared to the parameter requirements of baseline models, with differences ranging from 8.5K to 34.1M.

**Robust Stability Across Varied Tasks:** Our method showcases robust stability in tackling diverse tasks. It performs uniformly well across differing task scales (including those with varied activity durations), varied video characteristics (motion-focused and scene-focused video), and differing classification objectives (such as single-label and multi-label classifications). No baseline methods are currently able to match this level of comprehensive performance.

**Maintaining Video Context for Multiple Activities:** Within the multi-label dataset Charades, the  $mAP_{last}$  denotes the ability to recognize all activities in the video by its conclusion. Notably, Baselines 1 and 2 attained such accuracy by taking as input all video frames simultaneously. Our method achieves a higher accuracy based on the last frame and implicit memorization of past frames. Notably, our approach achieves 1.24 times the accuracy of Baseline 3, which employs LSTM for continuous processing. Results show that our CARS shows a better utilization of the hidden state.

Considering the inadequate accuracy demonstrated by Baselines 4 and 5, subsequent experimental evaluations will only involve Baselines 1, 2, and 3, along with ours.

Table 1. The accuracy and EDR results of different baselines. The #Param counts the parameters that need to be trained. Baselines 1, 2, 3, and our method have the same pre-trained clip with a parameter size of 149M.

Methods	#Param	FineGym99		FineGym288		Charades		
		Acc (%)	EDR (%)	Acc (%)	EDR (%)	mAP <sub>all</sub> (%)	mAP <sub>last</sub> (%)	EDR (%)
<b>B1</b> (Transformer-based)	<b>210.5K</b>	82.3	48.20	76.6	53.20	17.2	21.4	52
<b>B2</b> (ConvPooling-based)	<b>367.3K</b>	82.6	38.40	75.4	41.40	15.8	21	43.3
<b>B3</b> (LSTM-based)	<b>218K</b>	84.1	23.40	78.4	25.80	15.33	17.8	84
<b>B4</b> (MoviNet)	<b>2.1M</b>	19.7	41.60	13.9	44.20	3.9	5.8	<b>32</b>
<b>B5</b> (Mvitv2)	<b>34.3M</b>	6.4	<b>20.50</b>	3.1	<b>24.10</b>	5.3	7.3	99.9
<b>Ours</b>	<b>202K</b>	<b>86.1</b>	22.50	<b>81.3</b>	25.10	<b>18.4</b>	<b>22.1</b>	56.3

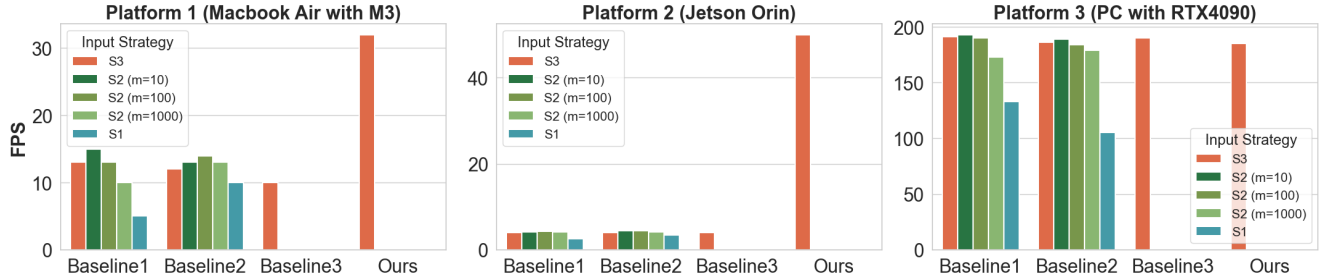


Figure 9. Processing speed of streaming video activity recognition with 10k frames on different platforms.

Table 2. Evaluation results on All-activity-in-one FineGym. (The parenthesized number of S2 signifies the window size, while 725 refers to the maximum frame count of a single activity.)

Method	Baseline 1					Baseline 3
Input Strategy	S3	S2 (10)	S2 (100)	S2 (725)	S1	S3
Acc (%)	4.1	6.6	4.2	6.2	-	7
Method	Baseline 2					Ours
Input Strategy	S3	S2 (10)	S2 (100)	S2 (725)	S1	S3
Acc (%)	4.7	11.8	13.4	11.3	7	<b>14.8</b>

### 4.3. Further Evaluation of Capabilities 1 & 2

We assess the continuous perception capability with the All-activity-in-one FineGym dataset, a 3.5-hour video described in Section 4.1. All baseline methods use the model trained on the FineGym99 dataset, whose accuracy evaluated on a single video clip is reported in Table 2. These methods are evaluated with different input strategies. For batch processing approaches (Baselines 1 and 2), we test all three strategies. Regarding streaming processing methods (our CARS and Baseline 3), we use the single frame feeding strategy (Strategy 3). Both our CARS and Baseline 3 benefit from the model’s memorization of past video frames. During continuous perception, each frame is processed only once without redundant input. The Acc metric is calculated by considering predictions of all video frames.

Baseline 1’s transformer structure results in slower processing as the input sequence grows. Therefore, Baseline 1 faced challenges during evaluation with input strategy 1

due to increasing input sequence length over time. Detailed system performance is provided in Figure 4.

Based on the results, we draw the following two conclusions. First, our CARS demonstrates the **best continuous perception ability** (*Capability 2*). It surpasses batch processing methods ranging from 0.5 to 10.7. Its accuracy is twice that of traditional LSTM-based baseline methods. Second, our approach can effectively **adapt to activities of varying scales** (*Capability 1*). In the hours-long video, activities lasted from tens of frames to hundreds of frames. Our CARS achieves the best accuracy, which outperforms the current sliding-window and state-assist methods.

### 4.4. Real-time Inference on Edge

We measure the system performance on three mobile platforms with two long video clips. The long video clips were excerpted from the All-activity-in-one FineGym dataset, one containing 10k frames and the other 100k frames. We conducted each experiment three times and calculated the average. In Figure 9, we present the system performance of different baselines processing 10k frame videos on the three platforms. Additionally, in Figure 4, we report the system performance of different baselines processing 100k frame videos on a PC equipped with an RTX4090. FPS is calculated by dividing the total number of video frames by the total processing time.

Our experimental findings are as follows.

**Recognizing the video stream in real time.** In Figure 9, it can be observed that our method achieves real-time processing (>30fps) on different platforms. Even on Macbook Air and Jetson, our speed is 2 to 20 times faster



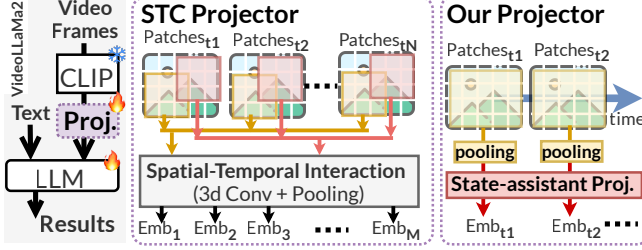


Figure 10. Applying our CARS into VideoLLaMa2 as a video encoder.

than the baseline methods. This improvement stems from two aspects. *Firstly, our streaming processing method* eliminates the need to use the model through all feeding or sliding window approaches. *Secondly, in terms of system implementation and optimization*, recall that mainstream frameworks, e.g., OpenClip, clip.cpp, and ONNXRuntime-GPU, lack support for using the CLIP model with Jetson GPU. Therefore, baselines can only utilize the CPU for computation. Our prototype can enable GPU computation on both Macbook Air and Jetson.

**No significant performance degradation as the frame number increases.** As shown in Figure 4, with an increase in input sequences, the performance of Baselines 1 and 2, using the all frame feeding and sliding windowed feeding strategy, significantly declined. When processing a 100k frame video, Baseline 1 drops to a speed of 9fps.

## 5. Case Study: Video Encoder for Large Video Models

In this section, we discuss how the design of our system, CARS, improves large video models in video activity recognition and understanding. As a case study, we analyze one of the SOTA large video models, VideoLLaMa2 [8] (left side of Figure 10). During video processing, VideoLLaMa2 first samples  $N$  frames from the video. These frames are then converted into  $M$  tokens by a multimodal projector (denoted as "Proj." in the figure). Simultaneously, the user's text prompt is tokenized, combined with the video tokens, and input into the LLM for inference.

### 5.1. Problem Analysis

VideoLLaMa2 introduces an STC projector as the projection layer. As shown in the middle part of Figure 10, the STC projector utilizes a *batch-based idea* to understand the video *without reducing the redundancy*. Specifically, it performs 3D convolutions on the feature of  $N$  sampled frames. The design of **the STC projector limits VideoLLaMa2's effectiveness and performance**. Therefore, it struggles to support higher sampling rates because 3D convolutions on a larger batch demand significant computational resources. As a result, only two versions of the model are available:

Table 3. Evaluation results on the VideoLLaMa2.

	VideoChatGPT Corr. (5-point)	ActivityNet Acc (%)	MSVD Acc (%)
VideoLLaMa2	1.95	38.46	44.6
Ours	<b>2.41</b>	<b>39.65</b>	<b>48.6</b>

one that processes 8 frames and another that processes 16 frames. Regardless of the video length or event scale, this fixed frame sampling inevitably reduces the model's accuracy.

### 5.2. Our design

We adopt the design of our CARS to build a new projection layer, named the CARS projector, which replaces the STC projector. This new projection utilizes our activity-aware state update to maintain the video context efficiently. Our state-assisted design can efficiently increase the sampling rate of the input video, far exceeding the existing designs with 8 or 16 frames, without increasing the processing time. Figure 10 (right) illustrates our design. When a video frame is input, the projector first processes the spatial information within the frame by applying mean pooling to patch embeddings. Next, our state-assistant module processes the input video, capturing relationships over time.

### 5.3. Experiments

**Implementation.** Using the official videollama2 codebase [6], we implemented our CARS projector. This projector consists of mean pooling, a linear layer with ReLU, and the history modeling layer of our CARS with a code dimension of 2048, followed by another linear layer with ReLU. The total parameter count of our projector is 450 M. For comparison, the STC projector with 8 frames has 1.8 B parameters, which is four times larger.

We fine-tuned and evaluated the model following the official guidelines. All hyperparameters were set to the official default values. During fine-tuning, only the large language model (LLM) and the projection layer were trained. We used the videoChatGPT dataset [25] for fine-tuning both the original model structure and our proposed model structure. All experiments were performed on a machine with eight A600 GPUs. Due to limited training resources, we used the 8-frame model as the baseline, while our method extended the training sample length to 128 frames.

**Results.** Testing was conducted on the videoChatGPT dataset (in-distribution), ActivityNet-QA [44] (zero-shot), and MSVD-QA [43] (zero-shot), and the results are reported in Table 3. For the VideoChatGPT dataset, correctness was measured on a 5-point scale. Our method outperformed the baseline by 0.46 points. On the other two zero-shot datasets, our approach achieved improvements of 1.19% and 4%, respectively. These results demonstrate that

our projector design effectively improves model accuracy, highlighting a new design concept for video projection for large video models.

## 6. Conclusion

Continuous video activity recognition in streaming video is important for complex multimodal human-computer interaction, e.g., embodied AI. However, achieving this on resource-limited edge devices is challenging. This paper proposes CARS, a state-assistant approach for continuous video activity recognition in streaming video. It consists of two key designs: activity spatial feature extraction to reduce spatial redundancy and activity-aware state update to maintain the video context effectively. Experimental results show that CARS can achieve real-time continuous video recognition on typical edge platforms. We believe that our CARS offers a novel idea for future streaming video processing.

## References

- [1] clip.cpp implementation. <https://github.com/monatis/clip.cpp#348b283>. 6
- [2] llama.cpp implementation. <https://github.com/ggerganov/llama.cpp>. 6
- [3] Mamba implementation. <https://github.com/mamba-org/mamba>. 6
- [4] Onnxruntime-gpu implementation. <https://pypi.org/project/onnxruntime-gpu/v1.18.1>. 6
- [5] Openclip implementation. [https://github.com/mlfoundations/open\\_clip/tree/v2.26.0](https://github.com/mlfoundations/open_clip/tree/v2.26.0). 6
- [6] Videollama2 implementation. <https://github.com/DAMO-NLP-SG/VideoLLaMA2>. 9
- [7] Guo Chen, Yifei Huang, Jilan Xu, Baoqi Pei, Zhe Chen, Zhiqi Li, Jiahao Wang, Kunchang Li, Tong Lu, and Limin Wang. Video mamba suite: State space model as a versatile alternative for video understanding. *arXiv preprint arXiv:2403.09626*, 2024. 1, 5
- [8] Zesen Cheng, Sicong Leng, Hang Zhang, Yifei Xin, Xin Li, Guanzheng Chen, Yongxin Zhu, Wenqi Zhang, Ziyang Luo, Deli Zhao, and Lidong Bing. Videollama 2: Advancing spatial-temporal modeling and audio understanding in video-llms. *arXiv preprint arXiv:2406.07476*, 2024. 2, 3, 5, 9
- [9] Jiafei Duan, Samson Yu, Hui Li Tan, Hongyuan Zhu, and Cheston Tan. A survey of embodied ai: From simulators to research tasks. *IEEE Transactions on Emerging Topics in Computational Intelligence*, 2022. 1, 2
- [10] Christoph Feichtenhofer, Haoqi Fan, Jitendra Malik, and Kaiming He. Slowfast networks for video recognition. In *ICCV*, 2019. 2
- [11] Samir Yitzhak Gadre, Kiana Ehsani, Shuran Song, and Roozbeh Mottaghi. Continuous scene representations for embodied ai. In *CVPR*, 2022. 1, 2
- [12] Alexander Greaves-Tunnell and Zaid Harchaoui. A statistical investigation of long memory in language and music. In *ICML*. PMLR, 2019. 5
- [13] Albert Gu and Tri Dao. Mamba: Linear-time sequence modeling with selective state spaces. *arXiv preprint arXiv:2312.00752*, 2023. 3, 5
- [14] Sepp Hochreiter and Jürgen Schmidhuber. Long short-term memory. *Neural computation*, 1997. 3, 6
- [15] Chao Huang, Like Zhang, Yanqing Jing, and Dajun Zhou. Efficient imitation learning for game ai. In *2020 IEEE Conference on Games*, 2020. 3
- [16] De-An Huang, Vignesh Ramanathan, Dhruv Mahajan, Lorenzo Torresani, Manohar Paluri, Li Fei-Fei, and Juan Carlos Niebles. What makes a video a video: Analyzing temporal information in video understanding models and datasets. In *CVPR*, 2018. 1
- [17] Boyuan Jiang, MengMeng Wang, Weihao Gan, Wei Wu, and Junjie Yan. Stm: Spatiotemporal and motion encoding for action recognition. In *ICCV*, 2019. 2, 3
- [18] Amlan Kar, Nishant Rai, Karan Sikka, and Gaurav Sharma. Adascan: Adaptive scan pooling in deep convolutional neural networks for human action recognition in videos. In *CVPR*, 2017. 3, 6
- [19] Dan Kondratyuk, Liangzhe Yuan, Yandong Li, Li Zhang, Mingxing Tan, Matthew Brown, and Boqing Gong. Movinets: Mobile video networks for efficient video recognition. In *CVPR*, 2021. 2, 6
- [20] Kunchang Li, Xinhao Li, Yi Wang, Yinan He, Yali Wang, Limin Wang, and Yu Qiao. Videomamba: State space model for efficient video understanding, 2024. 3, 5
- [21] Yan Li, Bin Ji, Xintian Shi, Jianguo Zhang, Bin Kang, and Limin Wang. Tea: Temporal excitation and aggregation for action recognition. In *CVPR*, 2020. 2, 3
- [22] Yanghao Li, Chao-Yuan Wu, Haoqi Fan, Karttikeya Mangalam, Bo Xiong, Jitendra Malik, and Christoph Feichtenhofer. Mvitv2: Improved multiscale vision transformers for classification and detection. In *CVPR*, 2022. 6
- [23] Ji Lin, Chuhan Gan, and Song Han. Tsm: Temporal shift module for efficient video understanding. In *ICCV*, 2019. 2, 3
- [24] Ilya Loshchilov and Frank Hutter. Decoupled weight decay regularization. *arXiv preprint arXiv:1711.05101*, 2017. 6
- [25] Muhammad Maaz, Hanoona Rasheed, Salman Khan, and Fahad Shahbaz Khan. Video-chatgpt: Towards detailed video understanding via large vision and language models. *arXiv preprint arXiv:2306.05424*, 2023. 9
- [26] Neelu Madan, Andreas Møgelmoose, Rajat Modi, Yogesh S Rawat, and Thomas B Moeslund. Foundation models for video understanding: A survey. *arXiv preprint arXiv:2405.03770*, 2024. 1
- [27] John Miller and Moritz Hardt. Stable recurrent models. *arXiv preprint arXiv:1805.10369*, 2018. 5
- [28] Bo Peng, Eric Alcaide, Quentin Anthony, Alon Albalak, Samuel Arcadinho, Stella Biderman, Huanqi Cao, Xin Cheng, Michael Chung, Matteo Grella, et al. Rwkv: Reinventing rnns for the transformer era. *arXiv preprint arXiv:2305.13048*, 2023. 3
- [29] Alec Radford, Jong Wook Kim, Chris Hallacy, Aditya Ramesh, Gabriel Goh, Sandhini Agarwal, Girish Sastry,

- Amanda Askill, Pamela Mishkin, Jack Clark, et al. Learning transferable visual models from natural language supervision. In *ICML*, 2021. 4
- [30] Dian Shao, Yue Zhao, Bo Dai, and Dahua Lin. Finegym: A hierarchical video dataset for fine-grained action understanding. In *CVPR*, 2020. 1, 3, 6
- [31] Alex Sherstinsky. Fundamentals of recurrent neural network (rnn) and long short-term memory (lstm) network. *Physica D: Nonlinear Phenomena*, 2020. 5
- [32] Xingjian Shi, Zhoung Chen, Hao Wang, Dit-Yan Yeung, Wai-Kin Wong, and Wang-chun Woo. Convolutional lstm network: A machine learning approach for precipitation nowcasting. *NeurIPS*, 2015. 3
- [33] Jerome Sieber, Carmen Amo Alonso, Alexandre Didier, Melanie N Zeilinger, and Antonio Orvieto. Understanding the differences in foundation models: Attention, state space models, and recurrent neural networks. *arXiv preprint arXiv:2405.15731*, 2024. 4
- [34] Gunnar A. Sigurdsson, Gül Varol, Xiaolong Wang, Ivan Laptev, Ali Farhadi, and Abhinav Gupta. Hollywood in homes: Crowdsourcing data collection for activity understanding. *ArXiv e-prints*, 2016. 6
- [35] Ombretta Strafforello, Klamer Schutte, and Jan Van Gemert. Are current long-term video understanding datasets long-term? In *ICCV*, 2023. 1, 2
- [36] Yutao Sun, Li Dong, Shaohan Huang, Shuming Ma, Yuqing Xia, Jilong Xue, Jianyong Wang, and Furu Wei. Retentive network: A successor to transformer for large language models. *arXiv preprint arXiv:2307.08621*, 2023. 3
- [37] Yunlong Tang, Jing Bi, Siting Xu, Luchuan Song, Susan Liang, Teng Wang, Daoan Zhang, Jie An, Jingyang Lin, Rongyi Zhu, et al. Video understanding with large language models: A survey. *arXiv preprint arXiv:2312.17432*, 2023. 1
- [38] Naftali Tishby, Fernando C Pereira, and William Bialek. The information bottleneck method. *arXiv preprint physics/0004057*, 2000. 4
- [39] Ashish Vaswani, Noam Shazeer, Niki Parmar, Jakob Uszkoreit, Llion Jones, Aidan N Gomez, Łukasz Kaiser, and Illia Polosukhin. Attention is all you need. *NeurIPS*, 2017. 6
- [40] Limin Wang, Yuanjun Xiong, Zhe Wang, Yu Qiao, Dahua Lin, Xiaoou Tang, and Luc Van Gool. Temporal segment networks: Towards good practices for deep action recognition. In *ECCV*, 2016. 3
- [41] Sinong Wang, Belinda Z Li, Madian Khabsa, Han Fang, and Hao Ma. Linformer: Self-attention with linear complexity. *arXiv preprint arXiv:2006.04768*, 2020. 3
- [42] Chao-Yuan Wu and Philipp Krahenbuhl. Towards long-form video understanding. In *CVPR*, 2021. 1
- [43] Dejing Xu, Zhou Zhao, Jun Xiao, Fei Wu, Hanwang Zhang, Xiangnan He, and Yueting Zhuang. Video question answering via gradually refined attention over appearance and motion. In *ACM Multimedia*, 2017. 9
- [44] Zhou Yu, Dejing Xu, Jun Yu, Ting Yu, Zhou Zhao, Yueting Zhuang, and Dacheng Tao. Activitynet-qa: A dataset for understanding complex web videos via question answering. In *AAAI*, 2019. 9
- [45] Jingyu Zhao, Feiqing Huang, Jia Lv, Yanjie Duan, Zhen Qin, Guodong Li, and Guangjian Tian. Do rnn and lstm have long memory? In *ICML*. PMLR, 2020. 5
- [46] Bolei Zhou, Alex Andonian, Aude Oliva, and Antonio Torralba. Temporal relational reasoning in videos. In *ECCV*, 2018. 1
- [47] Bolei Zhou, Alex Andonian, Aude Oliva, and Antonio Torralba. Temporal relational reasoning in videos. In *ECCV*, 2018. 3
- [48] Mohammadreza Zolfaghari, Kamaljeet Singh, and Thomas Brox. Eco: Efficient convolutional network for online video understanding. In *ECCV*, 2018. 1